1-26-2011

Proximity of the superconducting dome and the quantum critical point in the two-dimensional Hubbard model

S. X. Yang
Louisiana State University

H. Fotso
Louisiana State University

S. Q. Su
Louisiana State University

D. Galanakis
Louisiana State University

E. Khatami
Georgetown University

See next page for additional authors

Recommended Citation

Yang, S., Fotso, H., Su, S., Galanakis, D., Khatami, E., She, J., Moreno, J., Zaanen, J., & Jarrell, M. (2011). Proximity of the superconducting dome and the quantum critical point in the two-dimensional Hubbard model. *Physical Review Letters, 106* (4) https://doi.org/10.1103/PhysRevLett.106.047004

Proximity of the Superconducting Dome and the Quantum Critical Point in the Two-Dimensional Hubbard Model

S.-X. Yang, H. Fotso, S.-Q. Su, D. Galanakis, E. Khatami, J.-H. She, J. Moreno, J. Zaanen, and M. Jarrell

Phys. Rev. Lett. **106**, 047004 — Published 26 January 2011

DOI: 10.1103/PhysRevLett.106.047004

Proximity of the Superconducting Dome and the Quantum Critical Point in the Two-Dimensional Hubbard Model

S.-X. Yang[1], H. Fotso[1], S.-Q. Su[1,2], D. Galanakis[1], E. Khatami[3], J.-H. She[4], J. Moreno[1], J. Zaanen[4], and M. Jarrell[1]
[1]*Department of Physics and Astronomy, Louisiana State University, Baton Rouge, Louisiana 70803, USA*
[2]*Computer Science and Mathematics Division,Center for Nanophase Materials Sciences, Oak Ridge National Laboratory, Oak Ridge, Tennessee 37831-6164, USA*
[3]*Department of Physics, Georgetown University, Washington, District of Columbia, 20057, USA*
[4] *Instituut-Lorentz for Theoretical Physics, Universiteit Leiden, P.O. Box 9506, 2300 RA Leiden, The Netherlands*

We use the dynamical cluster approximation to understand the proximity of the superconducting dome to the quantum critical point in the two-dimensional Hubbard model. In a BCS formalism, T_c may be enhanced through an increase in the d-wave pairing interaction (V_d) or the bare pairing susceptibility (χ_{0d}). At optimal doping, where V_d is revealed to be featureless, we find a power-law behavior of $\chi_{0d}(\omega = 0)$, replacing the BCS log, and strongly enhanced T_c. We suggest experiments to verify our predictions.

Introduction- The unusually high superconducting transition temperature of the cuprates remains an unsolved puzzle, despite more than two decades of intense theoretical and experimental research. Central to the efforts to unravel this mystery is the idea that the high critical temperature is due to the presence of a quantum critical point (QCP) which is hidden under the superconducting dome [1]. Numerical calculations in the Hubbard model, which is accepted as the de-facto model for the cuprates, strongly support the case of a finite-doping QCP separating the low-doping region, found to be a non-Fermi liquid (NFL), from a higher doping Fermi-liquid (FL) region [2, 3]. Calculations also show that in the vicinity of the QCP, and for a wide range of temperatures, the doping and temperature dependence of the single-particle properties, such as the quasi-particle weight [2], as well as thermodynamic properties such as the chemical potential and the entropy, are consistent with marginal Fermi liquid (MFL) behavior [4]. This QCP emerges by tuning the temperature of a second-order critical point of charge separation transitions to zero and is therefore intimately connected to $q = 0$ charge fluctuations [5]. Finally, the critical doping seems to be in close proximity to the optimal doping for superconductivity as found both in the context of the Hubbard [5] and the t-J model [6]. Even though this proximity may serve as an indication that the QCP enhances pairing, the detailed mechanism is largely unknown.

In this Letter, we attempt to differentiate between two incompatible scenarios for the role of the QCP in superconductivity. The *first* scenario is the quantum critical BCS (QCBCS) formalism introduced by She and Zaanen (She-Zaanen) [7]. According to this, the presence of the QCP results in replacing the logarithmic divergence of the BCS pairing bubble by an algebraic divergence. This leads to a stronger pairing instability and higher critical temperature compared to the BCS for the same pairing interactions. The *second* scenario suggests that remnant fluctuations around the QCP mediate the pairing interaction [8, 9]. In this case the strength of the pairing interaction would be strongly enhanced in the vicinity of the QCP, leading to the superconducting instability. Here, we find that near the QCP, the pairing interaction depends monotonically on the doping, but the bare pairing susceptibility acquires an algebraic dependence on the temperature, consistent with the first scenario.

Formalism- In a conventional BCS superconductor, the superconducting transition temperature, T_c, is determined by the condition $V\chi_0'(\omega = 0) = 1$, where χ_0' is the real part of the $q = 0$ bare pairing susceptibility, and V is the strength of the pairing interaction. The transition is driven by the divergence of $\chi_0'(\omega = 0)$ which may be related to the imaginary part of the susceptibility via $\chi_0'(\omega = 0) = \frac{1}{\pi}\int d\omega \chi_0''(\omega)/\omega$. And $\chi_0''(\omega)$ itself can be related to the spectral function, $A_k(\omega)$, through

$$\chi_0''(x) = \frac{\pi}{N}\sum_{\zeta,k}\int d\omega A_k(\omega)A_k(\zeta x-\omega)\left(f(\omega-\zeta x)-f(\omega)\right) \tag{1}$$

where the summation of $\zeta \in \{-1,+1\}$ is used to anti-symmetrize $\chi_0''(\omega)$. In a FL, $\chi_0''(\omega) \propto N(\omega/2)\tanh(\omega/4T)$, and $\chi_0'(T) \propto N(0)\ln(\omega_D/T)$ with $N(0)$ the single-particle density of states at the Fermi surface and ω_D the phonon Debye cutoff frequency. This yields the well known BCS equation $T_c = \omega_D \exp(-1/(N(0)V)$. In the QCBCS formulation, the BCS equation is $V\chi'(\omega = 0) = 1$, where χ' is fully dressed by both the self energy and vertices associated with the interaction responsible for the QCP, but not by the pairing interaction V. In the Hubbard model the Coulomb interaction is responsible for both the QCP and the pairing, so this deconstruction is not possible. Thus, we will use the more common BCS T_c condition to analyze our results with $V\chi_0'(\omega = 0) = 1$ where χ_0' is dressed by the self energy but without vertex corrections. Since the QCP is associated with MFL behavior, we do not expect the bare bubble to display a FL logarithm divergence. Here, we explore the possibility that $\chi_0'(\omega = 0) \sim 1/T^\alpha$.

The two-dimensional Hubbard model is expressed as:

$$H = H_k + H_p = \sum_{k\sigma} \epsilon_k^0 c_{k\sigma}^\dagger c_{k\sigma} + U \sum_i n_{i\uparrow} n_{i\downarrow} \,, \qquad (2)$$

where $c_{k\sigma}^\dagger (c_{k\sigma})$ is the creation (annihilation) operator for electrons of wavevector k and spin σ, $n_{i\sigma} = c_{i\sigma}^\dagger c_{i\sigma}$ is the number operator, $\epsilon_k^0 = -2t\,(\cos(k_x) + \cos(k_y))$ with t being the hopping amplitude between nearest-neighbor sites, and U is the on-site Coulomb repulsion.

We employ the dynamical cluster approximation (DCA) [10] to study this model with a Quantum Monte Carlo (QMC) algorithm as the cluster solver. The DCA is a cluster mean-field theory which maps the original lattice onto a periodic cluster of size $N_c = L_c^2$ embedded in a self-consistent host. Spatial correlations up to a range L_c are treated explicitly, while those at longer length scales are described at the mean-field level. However the correlations in time, essential for quantum criticality, are treated explicitly for all cluster sizes. To solve the cluster problem we use the Hirsch-Fye QMC method [11, 12] and employ the maximum entropy method [13] to calculate the real-frequency spectra.

We evaluate the results starting from the Bethe-Salpeter equation in the pairing channel:

$$\begin{aligned} \chi(Q)_{P,P'} &= \chi_0(Q)_P \delta_{P,P'} \\ &\quad + \sum_{P''} \chi(Q)_{P,P''} \Gamma(Q)_{P'',P'} \chi_0(Q)_{P'} \end{aligned} \qquad (3)$$

where χ is the dynamical susceptibility, $\chi_0(Q)_P$ [$= -G(P+Q)G(-P)$] is the bare susceptibility, which is constructed from G, the dressed one-particle Green's function, Γ is the vertex function, and indices $P^{[\ldots]}$ and external index Q denote both momentum and frequency. The instability of the Bethe-Salpeter equation is detected by solving the eigenvalue equation $\Gamma\chi_0\phi = \lambda\phi$ [14] for fixed Q. By decreasing the temperature, the leading λ increases to one at a temperature T_c where the system undergoes a phase transition. To identify which part, χ_0 or Γ, dominates at the phase transition, we project them onto the d-wave pairing channel (which was found to be dominant [3, 15]). For χ_0, we apply the d-wave projection as $\chi_{0d}(\omega) = \sum_k \chi_0(\omega, q=0)_k g_d(k)^2 / \sum_k g_d(k)^2$, where $g_d(k) = (\cos(k_x) - \cos(k_y))$ is the d-wave form factor. As for the pairing strength, we employ the projection as $V_d = \sum_{k,k'} g_d(k) \Gamma_{k,k'} g_d(k') / \sum_k g_d(k)^2$, using Γ at the lowest Mastsubara frequency [16].

To further explore the different contributions to the pairing vertex, we employ the formally exact parquet equations to decompose it into different components [16, 17]. Namely, the fully irreducible vertex Λ, the charge (S=0) particle-hole contribution, Φ_c, and the spin (S=1) particle-hole contribution, Φ_s, through: $\Gamma = \Lambda + \Phi_c + \Phi_s$. Similar to the previous expression, one can write $V_d = V_d^\Lambda + V_d^c + V_d^m$, where each term is the d-wave component of the corresponding term. Using this scheme, we will be able to identify which component contributes the most to the d-wave pairing interaction.

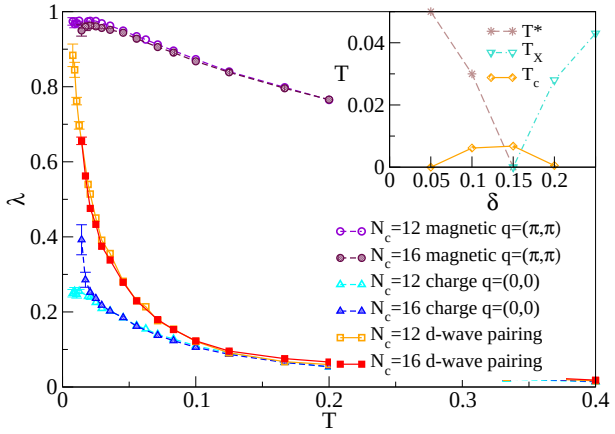

FIG. 1: (Color online) Plots of leading eigenvalues for different channels at the critical doping for $N_c = 12$ and $N_c = 16$ site clusters. The inset shows the phase diagram with superconducting dome, pseudogap T^* and FL T_X temperatures from Ref. [2]

Results- We use the BCS-like approximation, discussed above, to study the proximity of the superconducting dome to the QCP. We take $U = 6t$ ($4t = 1$) on 12 and 16 site clusters large enough to see strong evidence for a QCP near doping $\delta \approx 0.15$ [2, 4, 5]. We explore the physics down to $T \approx 0.11J$ on the 16 site cluster and $T \approx 0.07J$ on the 12-site cluster, where $J \approx 0.11$ [18] is the antiferromagnetic exchange energy. The fermion sign problem prevents access to lower T.

Fig. 1 displays the eigenvalues of different channels (pair, charge, magnetic) at the QC filling. The results for the two cluster sizes are nearly identical, and the pairing channel eigenvalue approaches one at low T, indicating a superconducting d-wave transition at roughly $T_c = 0.007$. However, in contrast to what was found previously [16], the $q = 0$ charge eigenvalue is also strongly enhanced, particularly for the larger $N_c = 16$ cluster, as it is expected from a QCP emerging as the terminus of a line of second-order critical points of charge separation transitions [5]. The inset shows the phase diagram, including the superconducting dome and the pseudogap T^* and FL T_X temperatures.

In Fig. 2, we show the strength of the d-wave pairing vertex V_d versus doping for a range of temperatures. Consistent with previous studies [19], we find that V_d falls monotonically with increasing doping. At the critical doping, $\delta_c = 0.15$, V_d shows no feature, invalidating the second scenario described above. The different components of V_d at the critical doping versus temperature are shown in the inset of Fig. 2. As the QCP is approached, the pairing originates predominantly from the spin channel. This is similar to the result of Ref. [16] where the pairing interaction was studied away from quantum crit-

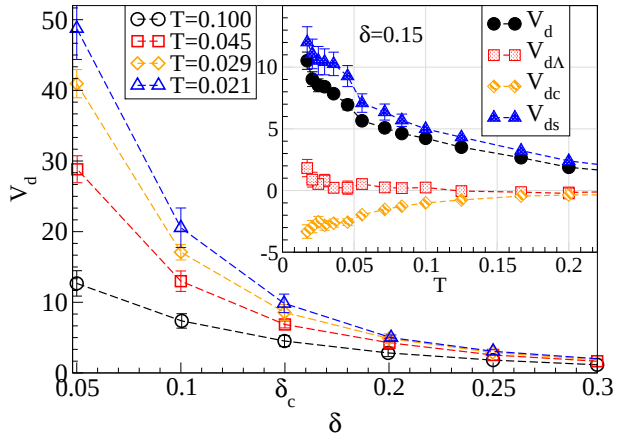

FIG. 2: (Color online) Plots of V_d, the strength of the d-wave pairing interaction for various temperatures with $U = 1.5$ ($4t = 1$) and $N_c = 16$. V_d decreases monotonically with doping, and shows no feature at the critical doping. In the inset are plots of the contributions to V_d from the charge V_d^c and spin V_d^s cross channels and from the fully irreducible vertex V_d^Λ versus T at the critical doping. As the temperature is lowered, $T \ll J \approx 0.11$, the contribution to the pairing interaction from the spin channel is clearly dominant.

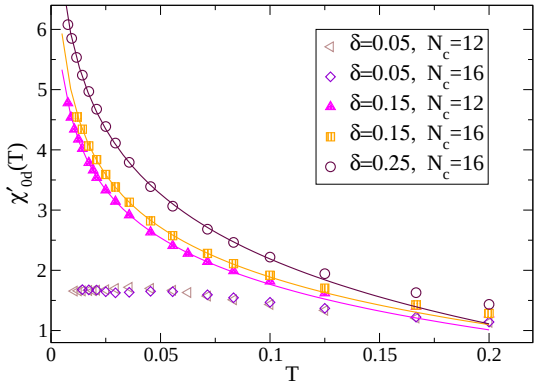

FIG. 3: (Color online) Plots of $\chi'_{0d}(\omega = 0)$, the real part of the bare d-wave pairing susceptibility, at zero frequency vs. temperature at three characteristic dopings. The solid lines are fits to $\chi'_{0d}(\omega = 0) = B/\sqrt{T} + A\ln(\omega_c/T)$ for $T < J$. In the underdoped case ($\delta = 0.05$), $\chi'_{0d}(\omega = 0)$ does not grow with decreasing temperature. At the critical doping ($\delta = \delta_c = 0.15$), $\chi'_{0d}(\omega = 0)$ shows power-law behavior with $B = 0.04$ for the 12 site, and $B = 0.09$ for the 16-site clusters (in both $A = 1.04$ and $\omega_c = 0.5$). In the overdoped region ($\delta = 0.25$), a log divergence is found, with $B = 0$ obtained from the fit.

icality.

In contrast, the bare d-wave pairing susceptibility χ_{0d} exhibits significantly different features near and away from the QCP. As shown in Fig. 3, in the underdoped region (typically $\delta = 0.05$), the bare d-wave pairing susceptibility $\chi'_{0d}(\omega = 0)$ saturates at low temperatures. However, at the critical doping, it diverges quickly with decreasing temperature, roughly following the power-law behavior $1/\sqrt{T}$, while in the overdoped or FL region it displays a log divergence.

To better understand the temperature-dependence of $\chi'_{0d}(\omega = 0)$ at the QC doping, we looked into $T^{1.5}\chi''_{0d}(\omega)/\omega$ and plotted it versus ω/T in Fig. 4. When scaled this way, the curves from different temperatures fall on each other such that $T^{1.5}\chi''_{0d}(\omega)/\omega = H(\omega/T) \approx (\omega/T)^{-1.5}$ for $\omega/T \gtrsim 9 \approx 4t/J$. For $0 < \omega/T < 4t/J$, the curves deviate from the scaling function $H(x)$ and show nearly BCS behavior, with $\chi''_{0d}(\omega)/\omega|_{\omega=0}$ which is weakly sublinear in $1/T$ as shown in the inset. The curves away from the critical doping (not displayed) do not show such a collapse. In the underdoped region ($\delta = 0.05$) at low frequencies, $\chi''_{0d}(\omega)/\omega$ goes to zero with decreasing temperature (inset). In the FL region ($\delta = 0.25$) $\chi''_{0d}(\omega)/\omega$ develops a narrow peak at low ω of width $\omega \approx T_X$ and height $\propto 1/T$ as shown in the inset.

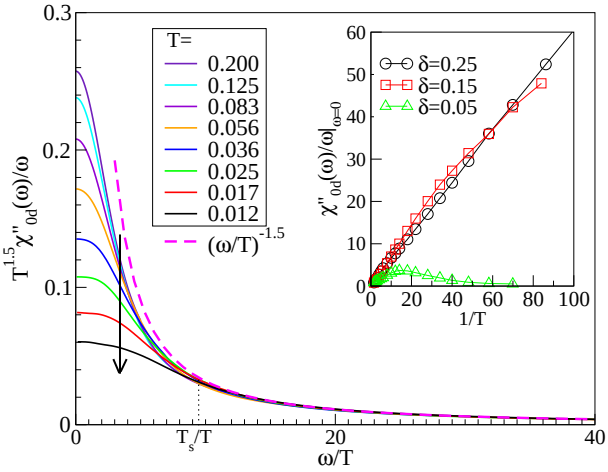

FIG. 4: (Color online) Plots of $T^{1.5}\chi''_{0d}(\omega)/\omega$ versus ω/T at the QC doping ($\delta = 0.15$) for $N_c = 16$. The arrow denotes the direction of decreasing temperature. The curves coincide for $\omega/T > 9 \approx (4t/J)$ defining a scaling function $H(\omega/T)$, corresponding to a contribution to $\chi'_{0d}(T) = \frac{1}{\pi}\int d\omega \chi''_{0d}(w)/w \propto 1/\sqrt{T}$ as found in Fig. 3. For $\omega/T > 9 \approx (4t/J)$, $H(\omega/T) \approx (\omega/T)^{-1.5}$ (dashed line). On the x-axis, we add the label $T_s/T \approx (4t/J)$, where T_s represents the energy scale where curves start deviating from H. The inset shows the unscaled zero-frequency result $\chi''_{0d}(\omega)/\omega|_{\omega=0}$ plotted versus inverse temperature.

Discussion- $\chi''_{0d}(\omega)/\omega$ reveals details about how the instability takes place. The overlapping curves found at the QC filling contribute a term $T^{-1.5}H(\omega/T)$ to $\chi''_{0d}(w)/w$ or $\chi'_{0d}(T) \propto 1/\sqrt{T}$ as found in Fig. 3. There is also a component which does not scale, especially at low frequencies. In fact, $\chi''_{0d}(\omega)/\omega$ at zero frequency increases more slowly than $1/T$ as expected for a FL. From this sublinear character, we infer that the contribution of the non-scaling part of $\chi''_{0d}(\omega)/\omega$ to the divergence of $\chi'_{0d}(T)$ is weaker than BCS and may cause us to overestimate A and underestimate B in the fits performed at the critical doping in Fig. 3. In addition, if $H(0)$ is finite,

it would contribute a term to $\chi'_{0d}(T)$ that increases like $1/T^{1.5}$, so $H(0) = 0$. From Eq. 1 we see that the contribution to $\chi''_{0d}(\omega)/\omega$ at small ω comes only from states near the Fermi surface. $H(0) = 0$ would indicate that the enhanced pairing associated with $\chi'_{0d}(T) \propto 1/\sqrt{T}$ is due to higher energy states. The vanishing of $\chi''_{0d}(\omega)/\omega$ in the pseudogap region ($\delta = 0.05$) for small frequency when $T \to 0$ indicates that around the Fermi surface, the dressed particles do not respond to a pair field. Or, perhaps more correctly, none are available for pairing due to the pseudogap depletion of electron states around the Fermi surface. Thus, even the strong d-wave interaction, seen in Fig. 2, is unable to drive the system into a superconducting phase. In the overdoped region, $\chi''_{0d}(\omega)/\omega$ displays conventional FL behavior for $T < T_X$, and the vanishing V_d suppresses T_c.

Together, the results for χ_{0d} and V_d shed light on the shape of the superconducting dome in the phase diagram found previously [5]. With increasing doping, the pairing vertex V_d falls monotonically. On the other hand, $\chi'_{0d}(T)$ is strongly suppressed in the low doping or pseudogap region and enhanced at the critical and higher doping. These facts alone could lead to a superconducting dome. Futhermore, the additional algebraic divergence of $\chi'_{0d}(T)$ seen in Fig. 3 causes the superconductivity to be enhanced even more strongly near the QCP where one might expect $T_c \propto (V_d B)^2$, with $B = \frac{1}{\pi}\int dx H(x)$, compared to the conventional BCS form in the FL region.

Similar to the scenario for cuprate superconductivity suggested by Castellani *et al.* [8], we find that the superconducting dome is due to charge fluctuations adjacent to the QCP related to charge ordering. However, we differ in that we find the pairing in this region is due to an algebraic temperature dependence of the bare susceptibility χ_{0d} rather than an enhanced d-wave pairing vertex V_d, and that this pairing interaction is dominated by the spin channel.

Our observation in the Hubbard model offers an experimental accessible variant of She-Zaanen's QCBCS. We use the bare pairing susceptibility χ_0 while She-Zaanen use the full χ, which includes all the effects of quantum criticality but not the correction from the pairing vertex (the pairing glue is added separately). This decomposition is not possible in numerical calculations or experiments since both quantum criticality and pairing originate from the Coulomb interaction. However, the effect of quantum criticality already shows up in the one-particle quantities, and the spectra have different behaviors for the three regions around the superconducting dome. She-Zaanen assume that $\chi''(\omega) \propto 1/\omega^\alpha$ for $T_s < \omega < \omega_c$, where ω_c is an upper cutoff, and that it is irrelevant ($\alpha < 0$), marginal ($\alpha = 0$), or relevant ($\alpha > 0$), respectively in the pseudo gap region, FL region and QCP vincity. We find the same behavior in χ_0 and we have the further observation that near the QCP $T_s \approx (4t/J)T$ and $\alpha = 0.5$.

Experiments combining angle-resolved photo emission (ARPES) and inverse photo emission results, with an energy resolution of roughly J, could be used to construct χ_{0d} and explore power law scaling at the critical doping. Since the energy resolution of ARPES is much better than inverse photo emission, it is also interesting to study $\chi''_{0d}(\omega)/\omega|_{\omega=0}$, which only requires ARPES data, but not inverse photo emission.

Conclusion- Using the DCA, we investigate the d-wave pairing instability in the two-dimensional Hubbard model near critical doping. We find that the pairing interaction remains dominated by the spin channel and is not enhanced near the critical doping. However, we find a power-law divergence of the bare pairing susceptibility at the critical doping, replacing the conventional BCS logarithmic behavior. We interpret this behavior by studying the dynamic bare pairing susceptibility which has a part that scales like $\chi''_{0d}(\omega)/\omega \sim T^{-1.5}H(\omega/T)$, where $H(\omega/T)$ is a universal function. Apparently, the NFL character of the QCP yields an electronic system that is far more susceptible to d-wave pairing than the FL and pseudogap regions. We also suggest possible experimental approaches to exploit this interesting behavior.

Acknowledgments- We would like to thank F. Assaad, I. Vekhter and E. W. Plummer for useful conversations. This research was supported by NSF DMR-0706379 and OISE-0952300. This research used resources of the National Center for Computational Sciences (Oak Ridge National Lab), which is supported by the DOE Office of Science under Contract No. DE-AC05-00OR22725. J.-H. She and J. Zaanen are supported by the Nederlandse Organisatie voor Wetenschappelijk Onderzoek (NWO) via a Spinoza grant.

[1] For a brief review, please see: D. M. Broun, Nature Phys. **4**, 170 (2008), S. Sachdev, Phys. Status Solidi B **247**, 537 (2010) and references therein.
[2] N. S. Vidhyadhiraja, et al., Phys. Rev. Lett. **102**, 206407 (2009).
[3] M. Jarrell, et al., EuroPhy. Letters, **56**, 563 (2001).
[4] K. Mikelsons, et al., Phys. Rev. B **80**, 140505(R) (2009).
[5] E. Khatami, et al., Phys. Rev. B **81**, 201101(R) (2010).
[6] K. Haule and G. Kotliar, Phys. Rev. B **76**, 092503 (2007).
[7] J.-H. She and J. Zaanen, Phys. Rev. B **80**, 184518 (2009).
[8] C. Castellani, et al., Z. Phy. B, **103**, 137-144 (1997).
[9] E.-G. Moon and A. Chubukov, J. Low Temp. Phys., **161**, 263 (2010).
[10] M. H. Hettler, et al., Phys. Rev. B **58**, R7475 (1998); M. H. Hettler, et al., Phys. Rev. B **61**,12739 (2000).
[11] J. E. Hirsch and R. M. Fye, Phys. Rev. Lett. **56**, 2521 (1986).
[12] M. Jarrell, et al., Phys. Rev. B **64**, 195130 (2001).
[13] M. Jarrell and J. E. Gubernatis, Phys. Rep. **269** No.3, 133 (1996).
[14] N. Bulut, et al., Phys. Rev. B **47**, 6157(R) (1993).
[15] T. A. Maier, et al., Phys. Rev. Lett. **95**, 237001 (2005).

[16] T. A. Maier, et al., Phys. Rev. Lett. **96**, 047005 (2006).
[17] S. X. Yang, et al., Phys. Rev. E **80**, 046706 (2009)
[18] N. S. Vidhyadhiraja, et al., Phys. Rev. Lett. **102**, 206407 (2009).
[19] T. A. Maier, et al., Phys. Rev. B **76**, 144516 (2007).
[20] P. Coleman and A. J. Schofield Nature **433**, 226 (2008).